

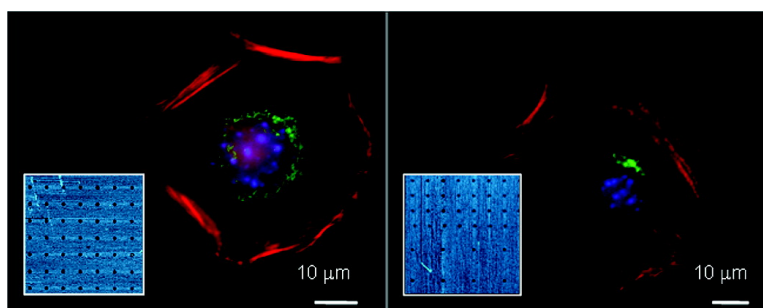
Communication

Asymmetric Peptide Nanoarray Surfaces for Studies of Single Cell Polarization

Diana K. Hoover, Eugene W. L. Chan, and Muhammad N. Yousaf

J. Am. Chem. Soc., **2008**, 130 (11), 3280-3281 • DOI: 10.1021/ja7111016m

Downloaded from <http://pubs.acs.org> on February 8, 2009



More About This Article

Additional resources and features associated with this article are available within the HTML version:

- Supporting Information
- Links to the 13 articles that cite this article, as of the time of this article download
- Access to high resolution figures
- Links to articles and content related to this article
- Copyright permission to reproduce figures and/or text from this article

[View the Full Text HTML](#)

Asymmetric Peptide Nanoarray Surfaces for Studies of Single Cell Polarization

Diana K. Hoover, Eugene W. L. Chan, and Muhammad N. Yousaf*

Department of Chemistry and the Carolina Center for Genome Science, University of North Carolina at Chapel Hill, Chapel Hill, North Carolina 27599-3290

Received December 11, 2007; E-mail: mnyousaf@email.unc.edu

Cell polarity is the ability to establish spatial, temporal, and functional asymmetry throughout the cell in response to cues from the local environment. This complex phenomenon plays a critical role in determining directed cell migration, ultimately impacting a wide range of biological processes including embryonic development, tissue repair, and the immune response.¹

In particular, cell polarity derived from cell adhesion through cell–cell and cell–extracellular matrix (ECM) interactions regulates many cell and tissue functions. Polarity within a cell can be generated through cell–cell interactions mediated by cell surface cadherins, which induce protein asymmetry at the intersecting membranes. Cell adhesion to ECM may also cause cell polarity by the nonuniform distribution of interactions between cell surface integrin receptors and ligands on the ECM.² These sites of external contact then recruit cytoskeletal and signaling proteins that in turn serve as a scaffold to recruit additional signaling proteins to generate an anisotropic subcellular nanoarchitecture that establishes cell polarity.³

In this report we develop a combined nanolithography, fluorescence microscopy of key organelles, and electroactive immobilization surface strategy to examine how the surface nanoadhesive environment directs the polarity of an adherent cell without the influence of cell–cell interactions.

In order to probe how cell polarity is established with the minimum amount of ligand mediated adhesions we developed a surface methodology based on dip pen nanolithography (DPN), a technique in which an atomic force microscope tip is used to deposit molecules in nanometer-sized features, to generate symmetric and asymmetric nanoarrays for studies of single cell polarity (Figure 1).⁴ Until now, there have been no studies using this powerful technique to examine how the precise nanoadhesive environment influences cell polarity.⁵ DPN was used to produce arrays of nanometer-sized spots of hydroquinone terminated alkanethiol on gold covered glass substrates. The remaining bare gold regions were backfilled with tetra(ethylene glycol) terminated alkanethiol. Electrochemical oxidation of the nanopatterned hydroquinone yields the corresponding quinone, which can react chemoselectively with soluble oxyamine-terminated ligands to precisely immobilize a variety of molecules to the surface for cell adhesion studies.⁶ The polarity of a cell can be experimentally measured through the systematic reorientation and alignment of several organelles in the cell including the nucleus, centrosome, and Golgi apparatus, which can be visualized using fluorescent dyes to map the direction of polarity.⁷

A symmetric nanoarray was produced via DPN deposition of hydroquinone terminated alkanethiol on a gold substrate in a 20 × 20 array of 500 nm diameter spots, with a pitch of 3 μm and a total area of 60 μm × 60 μm. An expanded region of the nanoarray is shown in the lateral force microscopy (LFM) image in Figure 2. The remaining bare gold regions were backfilled with tetra(ethylene

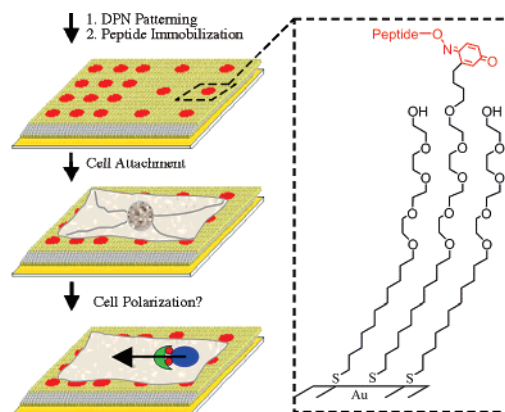


Figure 1. A schematic depiction of the production of asymmetric electroactive nanoarray patterns. DPN is used to pattern hydroquinone terminated alkanethiol in nanometer-sized spots. The remaining bare gold region is then backfilled with an inert tetra(ethylene glycol) terminated alkanethiol. Following electrochemical oxidation of the hydroquinone groups and chemoselective peptide immobilization, cells are seeded onto the surface. After a set period of time, the polarization of the cell is evaluated using fluorescent dyes targeting the nucleus (blue), centrosome (red), and golgi apparatus (green).

glycol) terminated alkanethiol (1 mM in ethanol, 12 h). The hydroquinone presenting nanoarrays were converted to the corresponding quinone through electrochemical oxidation, and an oxyamine terminated linear Arg-Gly-Asp (RGD) peptide (10 mM in PBS, 5 h) was then immobilized to the surface. The RGD peptide is found in the central binding region of fibronectin and is known to bind to integrin cell surface receptors.⁸

For cell adhesion on the nanoarray, 3T3 Swiss Albino mouse fibroblasts were added to the substrate for 8 h. Three fluorescent dyes targeting the nucleus, golgi apparatus, and the centrosome or actin cytoskeleton were used to visualize the cells. Giantin, a protein found in the membrane of the Golgi apparatus cisternae was chosen as a marker for that organelle.⁹ As can be seen in the fluorescent micrograph in Figure 2, the adherent cell adopts a morphology in which the nucleus is located approximately in the center of the cell. By determining the alignment vector of the Golgi apparatus relative to the nucleus and centrosome, we found no consistent directional polarity on the symmetric nanoarray for many cells ($n = 28$). In fact, almost all cells had a diffuse Golgi around the nucleus, a strong indicator of no polarity.

To further examine the influence of cell–ECM interactions on polarity we generated a single cell asymmetric nanoarray via DPN consisting of two sections of 500 nm diameter spots with a total area of 60 μm × 60 μm. The higher density region was a 20 × 10 array with a pitch of 3 μm, and the lower density region was a 10 × 5 array with a pitch of 6 μm (Figure 2). Linear RGD was immobilized, and fibroblasts were seeded and visualized as described above. A representative cell shown in the fluorescent

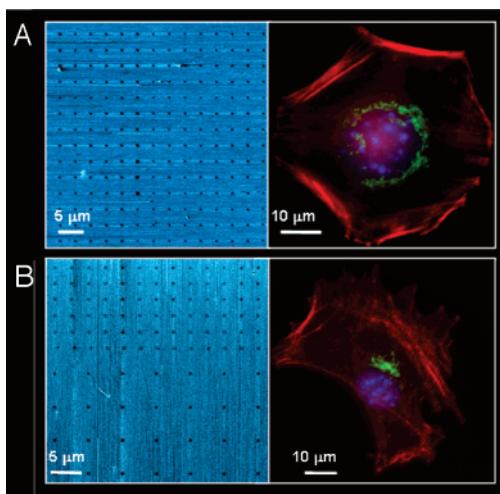


Figure 2. (A) (Left) Lateral force microscopy image of an expanded region of the control symmetric nanoarray (20×20 , 500 nm spots spaced $3 \mu\text{m}$ apart). (Right) Representative fluorescent micrograph of 3T3 Swiss Albino mouse fibroblast adhered to a symmetric nanoarray of immobilized linear RGD peptide. The diffuse distribution of the Golgi surrounding the nucleus indicates that the cell is not polarized on the symmetric nanoarray. (B) (Left) Lateral force microscopy image of an expanded area of an asymmetric nanoarray composed of two arrays of 500 nm spots 20×10 (spaced $3 \mu\text{m}$ apart) and 10×5 (spaced $6 \mu\text{m}$ apart). The vector between the concentrated Golgi with respect to the nucleus and centrosome indicates the cell is polarized toward the higher density region of the array. The cells were stained for nuclei (blue), Golgi apparatus (green), and actin (red).

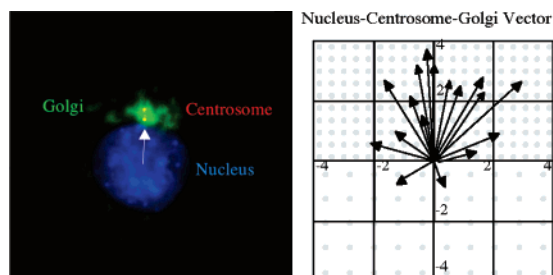


Figure 3. (Left) Polarity vector defining the distance between nucleus center, centrosome center, and Golgi center. (Right) Vector was used to define internal polarity on symmetric and asymmetric peptide nanoarrays. The axes represent distance in microns from the nucleus center to the centrosome center for cells ($n = 17$) on the asymmetric array. For asymmetric nanoarrays the net vector pointed toward the higher density adhesive region while there was no net polarity for cells on the symmetric adhesive array.

micrograph is polarized toward the higher density region of the asymmetric nanoarray, as evidenced by the relative positions of the nucleus and the concentrated Golgi apparatus. Statistical analysis of the two nanoarrays show the polarity vector for cells on the asymmetric array is directed to the higher density and therefore more adhesive region of the pattern, whereas there is no net vector in any direction on the symmetric array (Figure 3). This result clearly shows in the absence of cell–cell interactions a cell can be directly influenced by its nanoadhesive environment to polarize toward the higher density peptide ligands. We also generated symmetric arrays with decreasingly smaller spot sizes and found cells did not attach to spot sizes of <180 nm for linear RGD but did attach to the higher affinity ligand cyclic RGD (20×20 array with 180 nm spots spaced $3 \mu\text{m}$ apart).

Interestingly, when a higher affinity ligand (cyclic RGD) is immobilized to the asymmetric array no net directional polarity occurred (supplementary data). We also generated a doubly asymmetric array for single cell polarity studies consisting of a high-density region (500 nm spots spaced $3 \mu\text{m}$ apart) and a low-density region (250 nm spots spaced $6 \mu\text{m}$ apart) and found for cyclic RGD that the cell polarized again toward the higher density region (supplementary data). We hypothesize the affinity of the ligand and the spatial presentation of the ligands combine to govern the ability for the cell to polarize. To examine the role of focal adhesions in directing cell polarity we added a focal adhesion kinase knockout fibroblast cell line (FAK $-/-$) to the asymmetric arrays and found no net directional polarity on either linear or cyclic RGD nanoarrays. Furthermore, upon addition of nocodazole (100 nM, 30 min), a microtubule destabilizing drug, the polarized cells lost directional polarity on all asymmetric nanopatterns showing the microtubule network is critical for establishing directional polarity.

We also examined the spatial distribution of focal adhesion formation on the asymmetric nanoarrays for polarized cells.¹⁰ We found a significantly larger amount of focal adhesions corresponding to the higher density region on the asymmetric nanoarrays (Supporting Information).

In conclusion, we have demonstrated using dip pen nanolithography an investigation of single cell polarity at the level of the cellular nanoenvironment. We have shown that the spatial presentation of ligands and the affinity of ligands on the substrate have a substantial effect on the polarization of adherent fibroblasts. This was demonstrated through staining of the nucleus, centrosome, and the Golgi apparatus on symmetric and asymmetric peptide nanoarrays. Massively parallel DPN patterning in combination with the general electroactive immobilization strategy could lead to the development of single cell polarity arrays to screen for small molecule inhibitors or for fundamental investigations of cell adhesion and migration.¹¹

Acknowledgment. This work was supported by the Carolina Center for Cancer Nanotechnology Excellence (NCI).

Supporting Information Available: Experimental details and fluorescent micrographs of focal adhesion and polarity staining on symmetric and asymmetric linear and cyclic RGD surfaces. This material is available free of charge via the Internet at <http://pubs.acs.org>.

References

- (1) Ridley, A. J.; Schwartz, M. A.; Burridge, K.; Firtel, R. A.; Ginsberg, M. H.; Borisy, G.; Parsons, J. T.; Horwitz, A. R. *Science* **2003**, *302*, 1704–1709.
- (2) Yeaman, C.; Nelson, W. J. *Physiol. Rev.* **1999**, *79*, 73–98.
- (3) Jiang, X.; Bruzewicz, D. A.; Wong, A. P.; Piel, M.; Whitesides, G. M. *Proc. Natl. Acad. Sci. U.S.A.* **2005**, *102* (4), 975–978. Théry, M.; Racine, V.; Piel, M.; Pépin, A.; Dimitrov, A.; Chen, Y.; Sibarita, J.-P. *Proc. Natl. Acad. Sci. U.S.A.* **2006**, *103* (52), 19771–19776.
- (4) Piner, R. D.; Zhu, J.; Xu, F.; Mirkin, C. A. *Science* **1999**, *283*, 661–663.
- (5) Lee, K. B.; Mirkin, C. A.; Smith, J. C.; Mrksich, M. *Science* **2002**, *295*, 1702–1705.
- (6) Chan, E. W. L.; Yousaf, M. N. *J. Am. Chem. Soc.* **2006**, *128*, 15542–15546. Hoover, D. K.; Lee, E. J.; Yousaf, M. N. *ChemBioChem* **2007**, *8*, 1920–1923.
- (7) Kupfer, A.; Louvard, D.; Singer, S. J. *Proc. Natl. Acad. Sci. U.S.A.* **1982**, *79*, 2603–2607. Mellor, H. *Curr. Biol.* **2004**, *14*, R434–435.
- (8) Pierschbacher, M. D.; Ruoslahti, E. *Nature* **1984**, *309*, 30–33.
- (9) Linstedt, A. D.; Hauri, H.-P. *Mol. Biol. Cell* **1993**, *4*, 679–693.
- (10) Turner, C. E.; Burridge, K. *J. Cell Biol.* **1990**, *111*, 1059–1068.
- (11) Hodgson, L.; Chan, E. W. L.; Hahn, K. M.; Yousaf, M. N. *J. Am. Chem. Soc.* **2007**, *129*, 9264–9265.

JA711016M